

Flavor changing Flavon decay $\phi \rightarrow tc$ ($\phi = H_F, A_F$) at the High Luminosity Large Hadron Collider

M. A. Arroyo-Ureña,^{1,*} A. Fernández-Téllez,^{2,†} and G. Tavares-Velasco^{2,‡}

¹*Centro Interdisciplinario de Investigación y Enseñanza de la Ciencia (CIEC),
Benemérita Universidad Autónoma de Puebla,
C.P. 72570, Puebla, Pue., Mexico.*

²*Facultad de Ciencias Físico-Matemáticas,
Benemérita Universidad Autónoma de Puebla,
C.P. 72570, Puebla, Pue., Mexico.*

Abstract

We present a study of the flavor changing decays $\phi \rightarrow tc$ ($\phi = H_F, A_F$) of the CP -even and CP -odd scalar flavons at the large hadron collider and its next stage, the high-luminosity large hadron collider. The theoretical framework is an extension of the standard model that incorporates an extra complex singlet and invokes the Froggatt-Nielsen mechanism with an Abelian flavor symmetry. The projected exclusion and discovery regions in terms of the model parameters are reported. We find that A_F could be detected at the LHC by considering a reasonable scenario of the model parameter space. As far as H_F is concerned, we also found promising results that could be verified experimentally at the high-luminosity LHC.

* marcofis@yahoo.com.mx

† afernand@cfm.buap.mx

‡ gtv@cfm.buap.mx

I. INTRODUCTION

It is well known that the standard model (SM) has been successful in predicting results experimentally tested to a high accuracy, culminating with the recent discovery of a new scalar boson compatible with the SM Higgs boson [1, 2]. However, despite its success, some issues remain unexplained by the SM: the lack of a dark matter candidate, the hierarchy problem, unification, the flavor problem etc. This encourages the study of SM extensions. In the framework of the SM there are no tree-level flavor changing neutral currents (FCNC), which are, however, predicted by several SM extensions, being mediated by the Higgs boson or other new scalar or vector boson particles. In the context of these models, it is worth studying any signal that could give clues for new physics (NP), such as the widely studied process $\phi \rightarrow \tau\mu$, with ϕ a CP -even or CP -odd scalar boson [3–17]. FCNC signals can also arise from the top quark decays $t \rightarrow cX$ ($X = \phi, \gamma, g, Z, H$) [18–26], and from the less studied decay of a new heavy scalar boson into a top-charm quark pair [27], which could be searched at the LHC and the future high luminosity LHC (HL-LHC). The latter aims to increase the LHC potential capacity by reaching a luminosity up to $\mathcal{L} = 3000 \text{ fb}^{-1}$ around 2035 [28]. In this work we present a study of the $\phi \rightarrow tc$ decay in a SM extension that incorporates a complex singlet S_F via the Froggatt-Nielsen (FN) mechanism, which assumes that above some scale Λ_F a symmetry (perhaps of Abelian type $U(1)_F$) forbids the Yukawa couplings with the SM fermions charged under this symmetry; however, the Yukawa couplings can arise through non-renormalizable operators. The scalar spectrum of this model includes both a CP -even Flavon H_F and a CP -odd Flavon A_F . The former can mix with the SM Higgs boson when the flavor scale is of the order of a few TeVs. A detailed study of the Flavon phenomenology can be consulted in Refs. [29–33]. Our study not only could serve as a strategy for the Flavon search, but it can also be helpful to assess the order of magnitude of flavor violation mediated by this particles, which is an indisputable signature of physics beyond the SM.

The organization of this paper is as follows: in Sec. II we describe the most relevant theoretical aspects of the Froggatt-Nielsen singlet model (FNSM), which are necessary for our study. In Sec. III we obtain the constraints on the model parameters from the most recent experimental results on the Higgs boson coupling modifiers κ_i [34], the full decay width of the Higgs boson [35], anomalous magnetic dipole moment of the muon [36] and the perturbative limit. In addition, we include the current bound and the projections at the future colliders on $\text{BR}(t \rightarrow ch)$ in order to constrain the $g_{\phi tc}$ coupling. Sec. IV is devoted to the study signal $pp \rightarrow \phi \rightarrow tc(t \rightarrow \ell\nu_\ell b)$ and the potential background as well as the strategy used to search for the $\phi \rightarrow tc$ decay at the LHC and the HL-LHC. Finally, the conclusion are presented in Sec. V.

II. THE FROGGATT-NIELSEN COMPLEX SINGLET MODEL

We now focus on some relevant theoretical aspects of the FNSM. In Ref [37] a comprehensive analysis of the Higgs potential is presented, along with constraints on the parameter space from the constraints on the Higgs boson signal strengths and the oblique parameters, including a few benchmark scenarios. Also, the authors of Ref. [11] report a study of the lepton flavor violating (LFV) Higgs boson decay $h \rightarrow \ell_i \ell_j$ in the scenario where there is CP violation induced by a complex phase in the vacuum expectation value (VEV) of the complex singlet.

A. The scalar sector

In addition to the SM-like Higgs doublet, Φ , a FN complex singlet S_F is introduced. They are given by

$$\Phi = \begin{pmatrix} G^+ \\ \frac{1}{\sqrt{2}}(v + \phi^0 + iG_z) \end{pmatrix}, \quad (2.1)$$

$$S_F = \frac{1}{\sqrt{2}}(u + s + ip), \quad (2.2)$$

where v is the SM VEV and u is that of the FN complex singlet, whereas G^+ and G^z are identified with the pseudo-Goldstone bosons that become the longitudinal modes of the W^+ and Z gauge bosons.

We consider a scalar potential that respects a global $U(1)$ symmetry, with the Higgs doublet and the singlet transforming as $\Phi \rightarrow \Phi$ and $S_F \rightarrow e^{i\theta} S_F$. In general, such a scalar potential admits a complex VEV, namely, $\langle S_F \rangle_0 = u e^{-i\alpha}$, but in this work we consider the special case in which the Higgs potential is CP conserving, i.e. we consider the limit with vanishing phase. Such a CP -conserving Higgs potential is given by:

$$\begin{aligned} V = & -\frac{1}{2}m_1^2\Phi^\dagger\Phi - \frac{1}{2}m_{s_1}^2S_F^*S_F - \frac{1}{2}m_{s_2}^2(S_F^{*2} + S_F^2) \\ & + \frac{1}{2}\lambda_1(\Phi^\dagger\Phi)^2 + \lambda_s(S_F^*S_F)^2 + \lambda_{11}(\Phi^\dagger\Phi)(S_F^*S_F), \end{aligned} \quad (2.3)$$

where $m_{s_2}^2$ stands for a $U(1)$ -soft-breaking term, which is necessary to avoid the presence of a massless Goldstone boson, as will be evident below. Once the minimization conditions are applied, the following relations are obtained:

$$m_1^2 = v^2\lambda_1 + u^2\lambda_{11}, \quad (2.4)$$

$$m_{s_1}^2 = -2m_{s_2}^2 + 2u^2\lambda_s + v^2\lambda_{11}. \quad (2.5)$$

In this CP -conserving potential, the real and imaginary parts of the mass matrix do not mix. Thus, the mass matrix for the real components can be written in the (ϕ^0, s) basis as

$$M_S^2 = \begin{pmatrix} \lambda_1 v^2 & \lambda_{11} uv \\ \lambda_{11} uv & 2\lambda_s u^2 \end{pmatrix}. \quad (2.6)$$

The corresponding mass eigenstates are obtained via the standard 2×2 rotation

$$\begin{aligned} \phi^0 &= \cos \alpha h + \sin \alpha H_F, \\ s &= -\sin \alpha h + \cos \alpha H_F, \end{aligned} \quad (2.7)$$

with α a mixing angle. Here h is identified with the SM-like Higgs boson, with mass $m_h=125$ GeV, whereas the mass eigenstate H_F is the CP -even Flavon.

As for the mass matrix of the imaginary parts, it is already diagonal in the (G_z, p) basis:

$$M_P^2 = \begin{pmatrix} 0 & 0 \\ 0 & 2m_{s_2}^2 \end{pmatrix}, \quad (2.8)$$

where the physical mass eigenstate $A_F = p$ is the CP -odd Flavon. Both H_F and A_F are considered to be heavier than h .

B. Yukawa sector

The model, in addition to the new complex scalar singlet, also invokes the FN mechanism [38]. The effective FN $U(1)_F$ -invariant Lagrangian can be written as:

$$\begin{aligned} \mathcal{L}_Y &= \rho_{ij}^d \left(\frac{S_F}{\Lambda_F} \right)^{q_{ij}^d} \bar{Q}_{L_i} \Phi d_{R_j} + \rho_{ij}^u \left(\frac{S_F}{\Lambda_F} \right)^{q_{ij}^u} \bar{Q}_{L_i} \tilde{\Phi} u_{R_j} \\ &+ \rho_{ij}^\ell \left(\frac{S_F}{\Lambda_F} \right)^{q_{ij}^\ell} \bar{L}_{L_i} \Phi \ell_{R_j} + \text{H.c.}, \end{aligned} \quad (2.9)$$

which includes terms that become the Yukawa couplings once the $U(1)$ flavor symmetry is spontaneously broken. Here q_{ij}^f ($f = u, d, \ell$) denote the charges of each fermion type under some unspecified Abelian flavor symmetry, which help to explain the fermion mass hierarchy; ρ_{ij}^f are

dimensionless couplings seemingly of $\mathcal{O}(1)$, Λ_F represents the flavor scale and

$$\begin{aligned}\bar{Q}_{L_i}^T &= (u_{L_i}, d_{L_i}), \\ \bar{L}_{L_i}^T &= (\nu_{L_i}, \ell_{L_i}), \\ \tilde{\Phi} &= i\sigma^2 \Phi^*.\end{aligned}\tag{2.10}$$

We now write the neutral component of the Higgs field in the unitary gauge and use the first order expansion

$$\left(\frac{S_F}{\Lambda_F}\right)^{q_{ij}} = \left(\frac{u+s+ip}{\sqrt{2}\Lambda_F}\right)^{q_{ij}} \simeq \left(\frac{u}{\sqrt{2}\Lambda_F}\right)^{q_{ij}} \left[1 + q_{ij} \left(\frac{s+ip}{u}\right)\right],\tag{2.11}$$

along with Eqs. (2.2), (2.7) and (2.10). We also define $Y_{ij}^f = \rho_{ij}^f(u/\sqrt{2}\Lambda_F)^{q_{ij}^f}$, $\tilde{M}^f = (v/\sqrt{2})Y_{ij}^f$, $r_s = v/(\sqrt{2}u)$. In order to diagonalize the mass matrix \tilde{M}^f , the electroweak fields are redefined as

$$F_L \rightarrow U_L^f F_L, f_R \rightarrow U_R^f f_R \Rightarrow Y^f = U_L^{f\dagger} Y_{\text{diago}}^f U_R^f,\tag{2.12}$$

where $Y_{\text{diago}}^{f=\ell} = \frac{\sqrt{2}}{v} \text{diago}(m_e, m_\mu, m_\tau) = \frac{\sqrt{2}}{v} M^\ell$, analogously for the case of quarks. Thus, one gets the following Yukawa Lagrangian for the Higgs- and Flavon-fermion interactions:

$$\begin{aligned}\mathcal{L}_Y &= \frac{1}{v} [\bar{U} M^u U + \bar{D} M^d D + \bar{L} M^\ell L] (c_\alpha h + s_\alpha H_F) \\ &+ r_s [\bar{U}_i \tilde{Z}^u U_j + \bar{D}_i \tilde{Z}^d D_j + \bar{L}_i \tilde{Z}^\ell L_j] (-s_\alpha h + c_\alpha H_F + iA_F) + \text{H.c.},\end{aligned}\tag{2.13}$$

where $s_\alpha \equiv \sin \alpha$, $c_\alpha \equiv \cos \alpha$. A fact to highlight is that the intensity of the flavor violating (FV) couplings are encapsulated in the $\tilde{Z}_{ij}^f = U_L^{f\dagger} Z_{ij}^f U_R^f$ matrices. In the flavor basis, the Z_{ij}^f matrix elements are given by $Z_{ij}^f = \rho_{ij}^f(u/\sqrt{2}\Lambda_F)^{q_{ij}^f} q_{ij}^f$, which remains non-diagonal even after diagonalizing the mass matrices, thereby giving rise to FV scalar couplings. In addition to the Yukawa couplings, we also need the ϕVV ($V = W, Z$) couplings for our calculation, which can be extracted from the kinetic terms of the Higgs doublet and the complex singlet. In Table I we show the coupling constants for the interactions of the SM-like Higgs boson and the Flavons to fermions and gauge bosons.

III. CONSTRAINTS ON THE FNSM PARAMETER SPACE

To evaluate the decay widths and production cross-sections of the Flavons H_F and A_F , we need the bounds on the parameter space of our model, they are:

- The mixing angle α .

TABLE I: Couplings of the SM-like Higgs boson h and the Flavons H_F and A_F to fermion pairs and gauge boson pairs in the FNSM. Here $r_s = v/\sqrt{2}u$.

Vertex (ϕXX)	Coupling constant ($g_{\phi XX}$)
$hf_i\bar{f}_j$	$\frac{c_\alpha}{v}M_{ij}^f - s_\alpha r_s \tilde{Z}_{ij}^f$
$H_F f_i\bar{f}_j$	$\frac{s_\alpha}{v}M_{ij}^f + c_\alpha r_s \tilde{Z}_{ij}^f$
$A_F f_i\bar{f}_j$	$i r_s \tilde{Z}_{ij}^f$
hZZ	$\frac{gm_Z}{c_W}c_\alpha$
hWW	$gm_W c_\alpha$
$H_F ZZ$	$\frac{gm_Z}{c_W}s_\alpha$
$H_F WW$	$gm_W s_\alpha$

- The VEV of the FN complex singlet u .
- The matrix element \tilde{Z}_{tc} .
- The Flavon masses m_{H_F} and m_{A_F} .

A. Constraint on the mixing angle α and VEV of singlet u

It turns out that these parameters can be constrained via the Higgs boson coupling modifiers κ_j ($j = W, Z, g, b, \tau, \mu$) [34], which are defined for a given Higgs boson production mode $i \rightarrow h$ or decay channel $h \rightarrow j$ as

$$\kappa_i^2 = \sigma_i/\sigma_i^{\text{SM}} \quad \text{or} \quad \kappa_j^2 = \Gamma_j/\Gamma_j^{\text{SM}}, \quad (3.1)$$

where σ_i^{SM} (Γ_j^{SM}) stands for the pure SM contributions, whereas σ_i (Γ_j) includes new physics contributions.

Figure 1(a) shows the $c_\alpha - u$ plane, where each colored area represents the allowed regions by κ_j considering the expected results at the HL-LHC at a confidence level of 2σ . Besides, in the same plot, the intersection of all κ'_j s is included, which coincides with κ_τ since the latter is the most restrictive. Meanwhile, we present separately in Fig. 1(b) the intersection of all κ'_j s and the allowed region by both the perturbative limit applied on the parameter of the potential $\lambda_s = (m_{A_F}^2 + c_\alpha^2 m_{H_F}^2 + m_h^2 s_\alpha^2)/(2u^2) \leq 4\pi$ and the current discrepancy between the experimental measurement and the SM theoretical prediction [36] of the anomalous magnetic dipole moment given by

$$\Delta a_\mu = (25.1 \pm 5.9) \times 10^{-10}, \quad (3.2)$$

$$\Delta a_\mu^{\text{FNSM}} \approx \frac{m_\mu}{16\pi^2} \sum_{\phi=h, H_F, A_F} \sum_{\ell=\mu, \tau} \frac{m_\ell g_{\phi\mu\ell}^2}{m_\phi} \left(2 \ln \left(\frac{m_\phi^2}{m_\ell^2} \right) - 3 \right).$$

We notice in Fig. 1(b) that c_α is close to unity, this is to be expected because the dominant term of the $g_{hf_i\bar{f}_i}$ coupling in Table I is proportional to c_α . When $c_\alpha = 1$, the SM case is recovered. As far as the VEV of the FN complex singlet is concerned, it is a lower limit imposed by the perturbative limit; the most stringent is when $m_{A_F} = m_{H_F} = 1000$ GeV, $u \geq 281$ GeV. The exploration of the muon anomalous magnetic dipole moment help us to find a upper limit on $u \leq 1100$ GeV, in addition to imposing a lower limit on $c_\alpha \geq 0.995$. We also explored the total decay width of the Higgs boson in order to find additional constrains on the mixing angle α and u , however this observable is not restrictive.

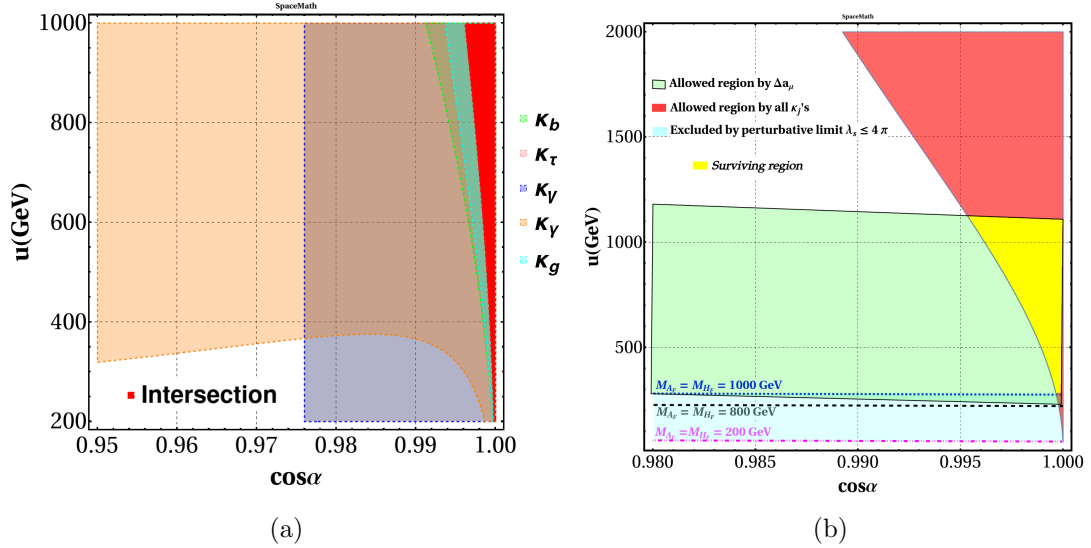


FIG. 1: (a) Allowed regions by all κ_j coupling modifiers in the $c_\alpha - u$ plane, where $V = Z, W$; (b) Only intersection of κ'_j 's and excluded zone by perturbative limit.

B. Constraint on \tilde{Z}_{tc}

So far, we only have considered the bound on the diagonal couplings; however, we need a bound on the \tilde{Z}_{tc} matrix element in order to evaluate the $\phi \rightarrow tc$ decay. To our knowledge, there are no processes from which we can extract a stringent bound on \tilde{Z}_{tc} , but we can assess its order of magnitude by considering the upper limits $\text{BR}(t \rightarrow ch) < 1.1 \times 10^{-3}$ [35]. We also consider the prospect for the branching ratio $\text{BR}(t \rightarrow ch) < 4.3 \times 10^{-5}$ searches at the FCC-hh [39]. This is shown in Fig. 2.

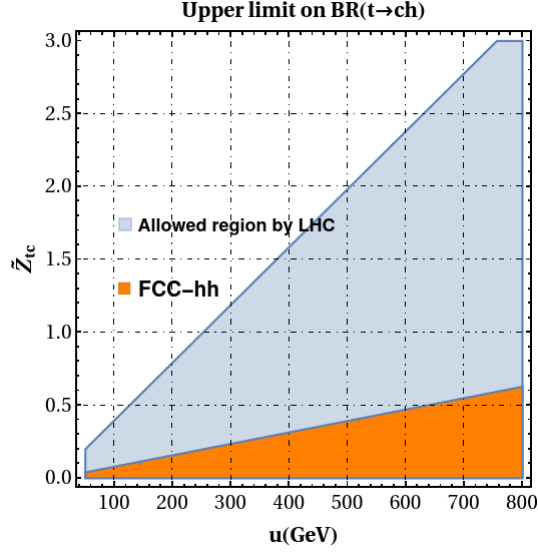


FIG. 2: Allowed region in the u - \tilde{Z}_{tc} plane from the current bound on $\text{BR}(t \rightarrow ch) < 1.1 \times 10^{-3}$ (blue color) and the projection at the FCC-hh (orange color).

TABLE II: Model parameter values considered in the numerical analysis.

Parameter	Value
c_α	0.999
u	600 and 1000 (GeV)
\tilde{Z}_{tt}	0.5
\tilde{Z}_{bb}	0.1
\tilde{Z}_{tc}	0.05, 0.2 and 0.45
$\tilde{Z}_{\tau\tau}$	0.1 [14]
$\tilde{Z}_{\mu\mu}$	10^{-3} [14]
$\tilde{Z}_{\tau\mu}$	0.35
m_{A_F}	0.2 – 1 (TeV)
m_{H_F}	0.2 – 1 (TeV)

As for the bounds on the $\tilde{Z}^{\ell\ell}$ diagonal matrix elements, we use those obtained in Ref. [14]. We summarize in Table II the values of the FNSM parameters used in the evaluations; while in Table III we define three benchmark points to be used in the Monte Carlo simulation.

TABLE III: Benchmark points used in the Monte Carlo simulation.

Benchmark points (BMP)
BMP1: $\tilde{Z}_{tc} = 0.45$, $u = 600, 1000$ GeV
BMP2: $\tilde{Z}_{tc} = 0.2$, $u = 600, 1000$ GeV
BMP3: $\tilde{Z}_{tc} = 0.05$, $u = 600, 1000$ GeV

IV. SEARCH FOR $\phi \rightarrow tc$ DECAYS AT THE HL-LHC

A. Flavon decays

We now present the behavior of the branching ratios of the main Flavon decay channels, which were obtained via our own `Mathematica` package so-called `SpaceMath` [40], that implements the analytical expressions for the corresponding decay widths. A cross-check was done by comparing our results with those obtained via `CalcHEP` [41], in which we implemented the corresponding Feynman rules via the `LanHEP` package [42]. In Fig. 3 we show the branching ratios of the CP -odd Flavon A_F as functions of its mass m_{A_F} ; we use the parameter values of Table II. As A_F does not couple to gauge bosons at tree-level, its dominant decay modes are $A_F \rightarrow t\bar{t}$, $A_F \rightarrow \tau^-\mu^+$, and $A_F \rightarrow t\bar{c}$, with a branching ratio at the $\mathcal{O}(0.1)$ level for masses of the Flavon A_F in the $200 \leq m_{A_F} \leq 1000$ GeV. Other interesting channels such as $A_F \rightarrow gg$ and $A_F \rightarrow b\bar{b}$ search a branching ratio of $\mathcal{O}(10^{-3}) - \mathcal{O}(10^{-2})$.

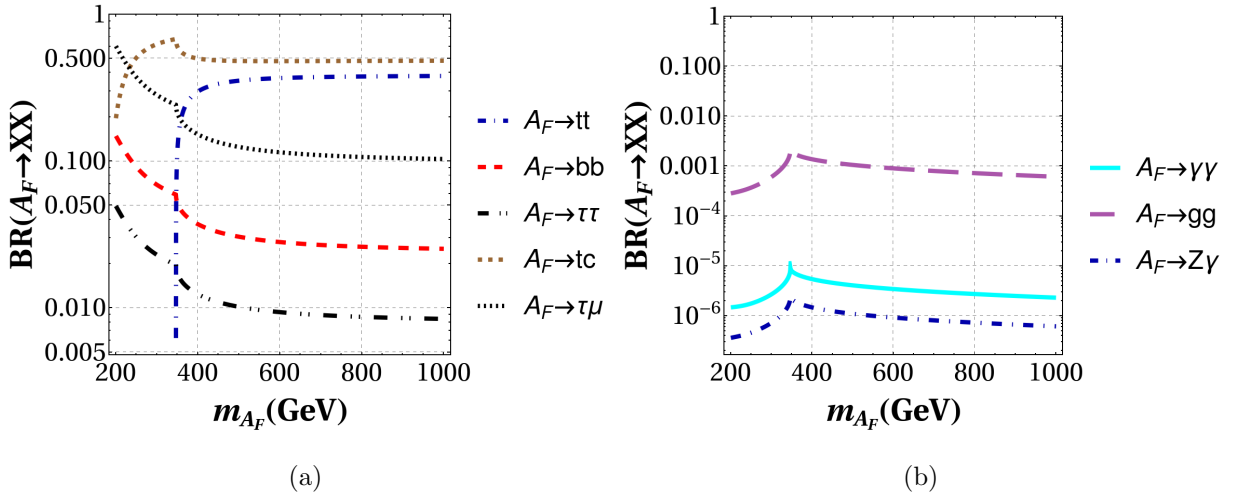


FIG. 3: Branching ratios of the two-body decay modes of a CP -odd flavon as a function of its mass for the parameter values of Table II ($u = 1000$ GeV and $\tilde{Z}_{tc} = 0.45$).

As far as the CP -even Flavon H_F is concerned, the branching ratios for their main decay

channels are presented in Fig. 4, for the same parameter values used for the A_F decays. We observe that the dominant H_F decay channels are $H_F \rightarrow \tau^- \mu^+$ and $H_F \rightarrow t\bar{c}$ for $m_{H_F} \leq 2m_{top}$, with branching ratios of order $\mathcal{O}(10^{-1})$. Another important channel is $H_F \rightarrow hh(h \rightarrow \gamma\gamma, h \rightarrow b\bar{b})$ which was studied by one of the authors of this project in Ref. [43]. Conversely, when $m_{H_F} \geq 2m_{top}$, the dominant channels are $H_F \rightarrow t\bar{t}$, W^+W^- , ZZ and $\tau^- \mu^+$. Other decay modes such as $H_F \rightarrow b\bar{b}$, $H_F \rightarrow \tau^- \tau^+$, $H_F \rightarrow \gamma\gamma$ and $H_F \rightarrow gg$ have branching ratios ranging from 10^{-6} to 10^{-3} , whereas the decays $H_F \rightarrow Z\gamma$ and $H_F \rightarrow \mu\mu$ are very suppressed.

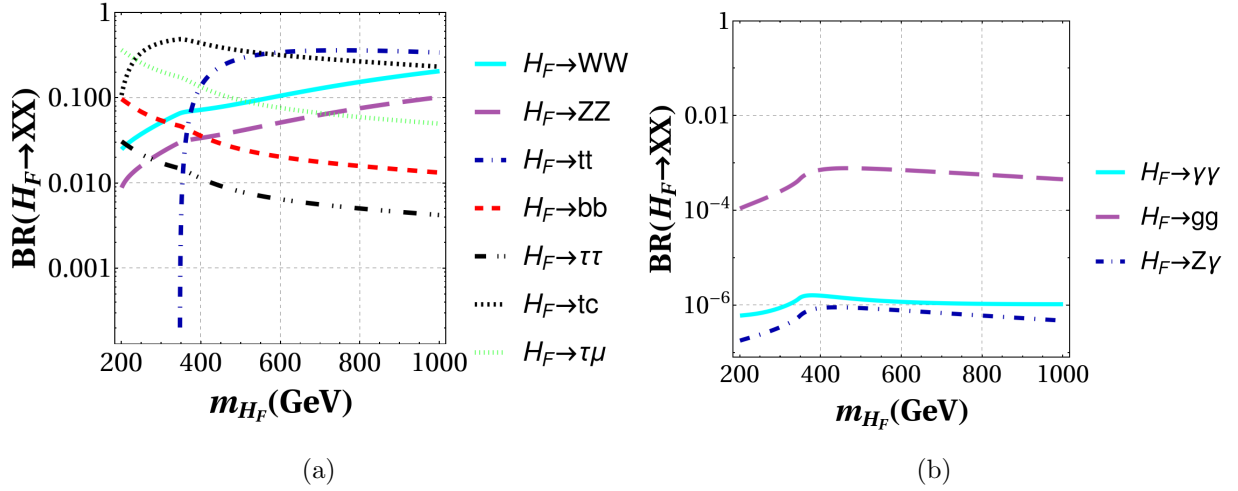


FIG. 4: Branching ratios of the two-body decay modes of a CP -even flavon as a function of its mass for the parameter values of Table II ($u = 1000$ GeV and $\tilde{Z}_{tc} = 0.45$).

B. Events

In this section we now present a Monte Carlo analysis for the production of both the H_F and the A_F Flavons at the LHC via gluon fusion $gg \rightarrow \phi$ ($\phi = H_F, A_F$), followed by the FCNC decay $\phi \rightarrow tc$. We apply realistic kinematic cuts and consider tagging and miss tagging efficiencies. We then obtain the statistical significance, which could be experimentally confirmed.

We present in Fig. 5 the number of events produced $\sigma(gg \rightarrow \phi \rightarrow tc(t \rightarrow \ell\nu_\ell b)) \times \mathcal{L}$ ($\equiv \mathcal{N}_\phi$), where $\mathcal{L} = 300 \text{ fb}^{-1}$ is the integrated luminosity at the final stage of the LHC. For this computation, we use CalCHEP [41] with the CT10 parton distribution functions [44]. We note that for both Flavon masses m_ϕ , \mathcal{N}_ϕ is similar in the $400 \leq m_\phi \leq 1000$ GeV interval. Meanwhile, for masses in the range $200 \leq m_\phi \leq 350$ GeV, $\mathcal{N}_{A_F} \approx 3\mathcal{N}_{H_F}$. These results are encouraging since similar statistical significance will be obtained, despite different kinematic behaviors.

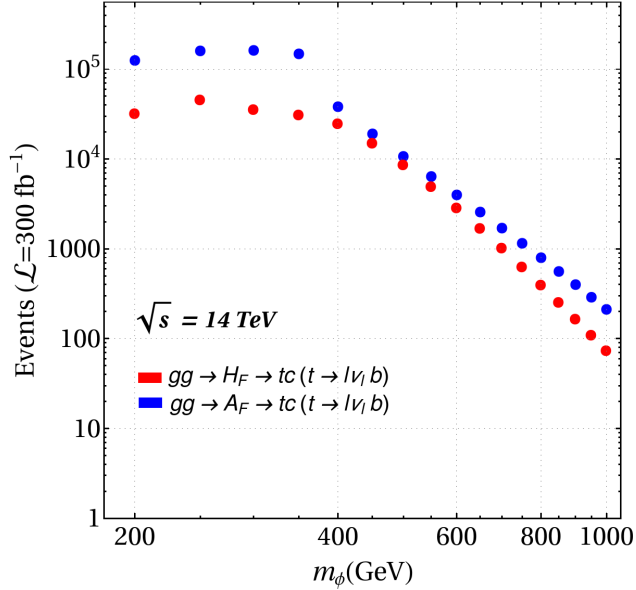


FIG. 5: Number of events produced for the process $gg \rightarrow \phi \rightarrow tc (t \rightarrow \ell \nu_\ell b)$ as a function of the Flavon mass m_ϕ at $\sqrt{s}=14$ TeV with an integrated luminosity of $\mathcal{L} = 300 \text{ fb}^{-1}$.

1. Kinematic cuts

We now turn to the Monte Carlo simulation, for which we use **Madgraph5** [45], with the corresponding Feynman rules generated via **LanHEP** [42] for a **UFO** model [46]. To perform shower and hadronization we use **Pythia8** [47].

The signal and the main background events are as follows:

- **SIGNAL:** The signal is $gg \rightarrow \phi \rightarrow tc \rightarrow b\ell\nu_\ell c$ with $\ell = e, \mu$. We generated 10^5 events scanning over $m_\phi \in [200, 1000]$ TeV and considered the parameter values of Table II.
- **BACKGROUND:** The dominant SM background arises from the final states $Wjj + Wb\bar{b}$, $tb + tj$ and $t\bar{t}$, in which either one of the two leptons is missed in the semi-leptonic top quark decays or two of the four jets are missed when one of the top quarks decays semi-leptonically.

In Fig. 6 we present the kinematic distributions generated both by the background processes and the decay of A_F for $m_{A_F} = 200$ GeV, namely, the transverse momentum of the particles produced by the decay of the top quark: (a) leading b-jet, (b) the charged lepton, (c) the missing energy transverse (MET) due to the neutrino in the final state is displayed. The transverse momentum of the leading jet is shown in (d). Finally, the transverse masses of the top quarks and CP-odd Flavon are depicted in (e) and (f). Meanwhile, in Figs. 7, 8, 9 shows the same as in Fig. 6 but only for the signal to $m_{A_F} = 200, 400, 900$ GeV.

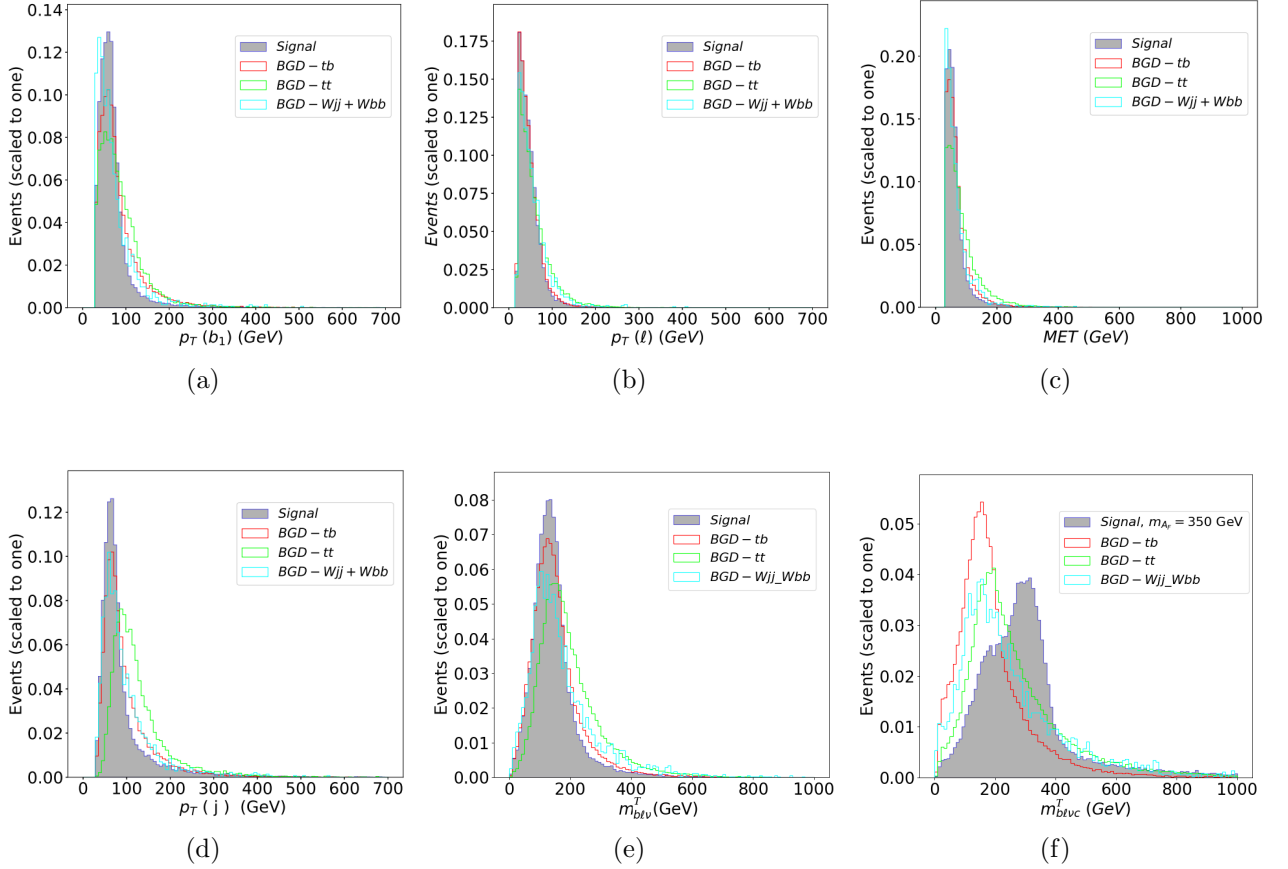


FIG. 6: Normalized transverse momentum distributions associated to the top decay: (a) leading b-jet, (b) leading charged lepton; (c) tranverse missing energy due to undetected neutrinos; (d) transverse momentum distribution of the c-jet; (e) top quark transverse mass ($m_{b\ell\nu}^T$) and (f) CP-odd Flavon transverse mass ($m_{b\ell\nu c}^T$) considering $m_{A_F} = 350$ GeV.

The kinematic cuts imposed to study a possible evidence of the $\phi \rightarrow tc$ ($m_\phi = 200$ GeV) at the LHC are as follows.

1. We require two jets with $|\eta^j| < 2.5$ and $p_T^j > 30$ GeV, one of them is tagged as a b-jet.
2. We require one isolated lepton (e or μ) with $|\eta^\ell| < 2.5$ and $p_T^\ell > 20$ GeV.
3. Since an undetected neutrino is included in the final state, we impose the cut $MET > 30$ GeV.
4. Finally, we impose a cut on the transverse masses $m_{b\ell\nu c}^T$ and $m_{b\ell\nu}^T$ as follows

- $0.8m_{A_F} < m_{b\ell\nu c}^T < 1.2m_{A_F},$

- $0.8m_{\text{top}} < m_{b\ell\nu}^T < 1.2m_{\text{top}}$.

The kinematic analysis was done via **MadAnalysis5** [48] and for detector simulations we use **Delphes** [49]. As far as the jet reconstruction, we use the jet finding package **FastJet** [50] and the anti- k_T algorithm [51]. We include also the tagging and mis-tagging efficiencies b -tagging efficiency $\epsilon_b = 90\%$ and to account for the probability that a c -jet is miss tagged as a b -jet we consider $\epsilon_c = 10\%$, whereas for any other jet we use $\epsilon_j = 1\%$.

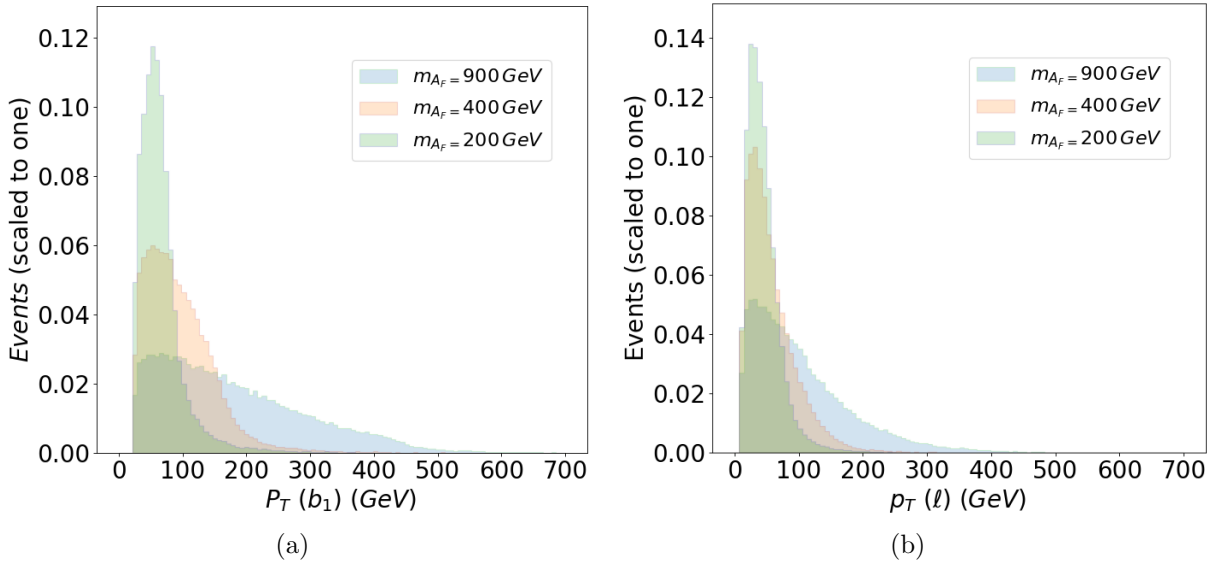


FIG. 7: Normalized distributions generated by the decay of A_F for $m_{A_F} = 200, 400, 900 \text{ GeV}$. Transverse momentum of (a) leading b-jet and (b) leading charged lepton.

We now compute the signal significance $\mathcal{S} = N_S / \sqrt{N_S + N_B}$, where N_S (N_B) are the number of signal (background) events once the kinematic cuts were applied. We show in Figs. 10-12 the contour plots of the signal significance as a function of m_{A_F} and the integrated luminosity for the BMP1-BMP3, respectively, as shown in Table III. The results for the case of the CP -even Flavon H_F , as well as the **MadGraph** files, will be shown upon request.

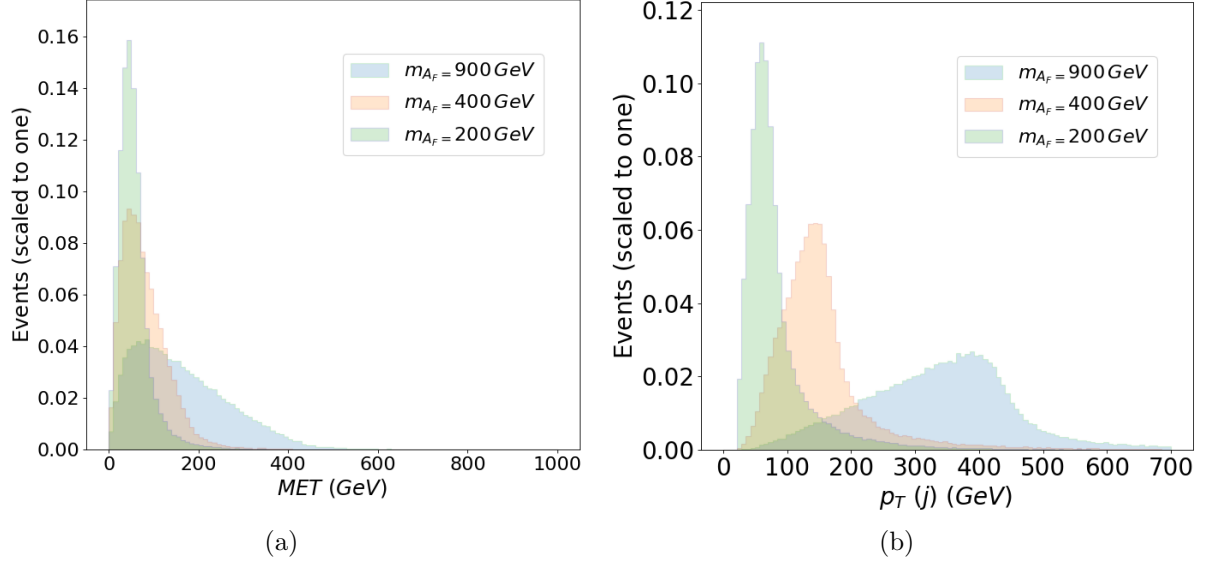


FIG. 8: Normalized distributions generated by the decay of A_F for $m_{A_F} = 200, 400, 900$ GeV. (a) transverse missing energy due to undetected neutrino, (b) transverse momentum distribution of the c-jet.

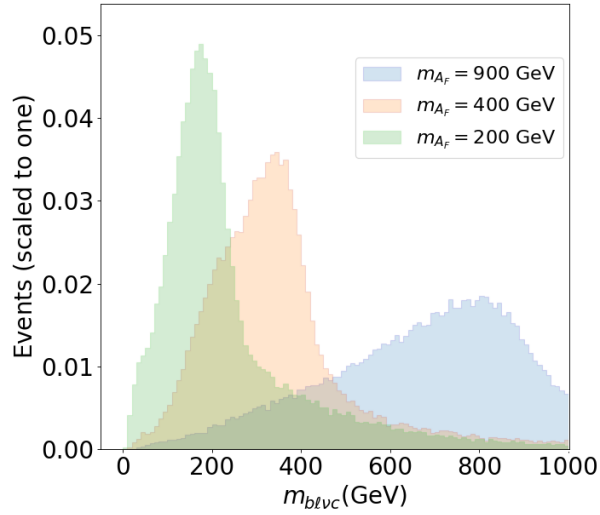


FIG. 9: Reconstructed CP-odd Flavon mass for $m_{A_F} = 200, 400, 900$ GeV.

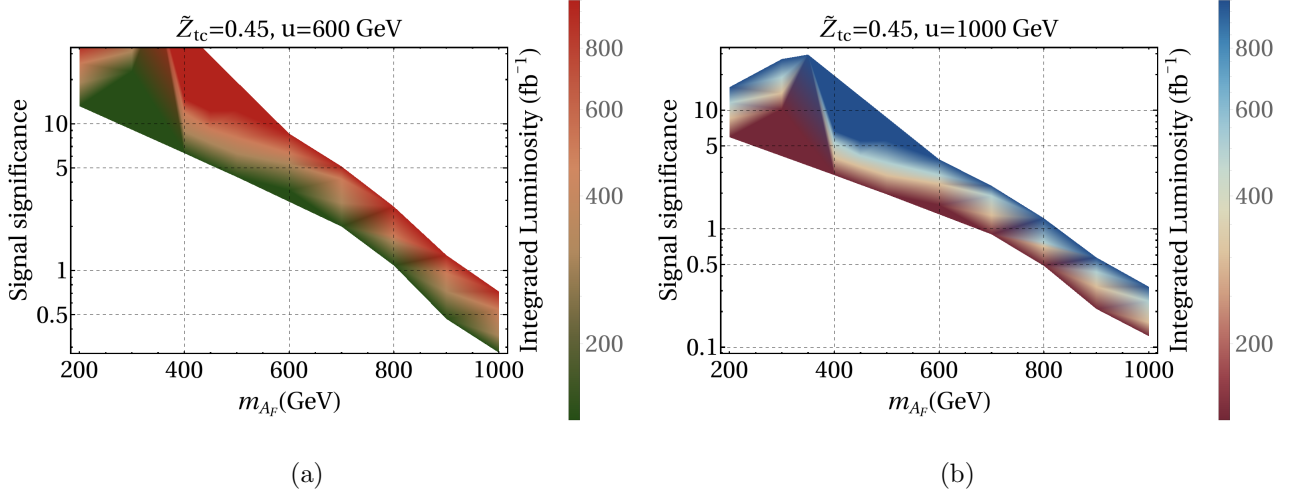


FIG. 10: Contour plots for the signal significance as a function of the integrated luminosity and the CP -odd flavon mass, m_{A_F} .

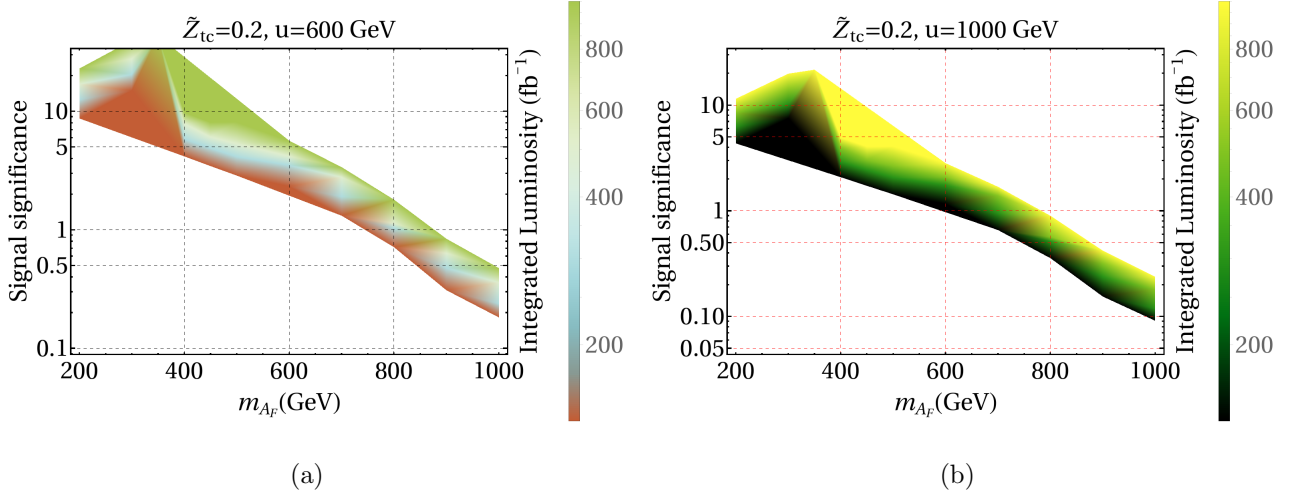


FIG. 11: Contour plots for the signal significance as a function of the integrated luminosity and the CP -odd flavon mass, m_{A_F} .

V. CONCLUSIONS

We study an extension of the SM with a complex singlet that invokes the Froggatt-Nielsen mechanism with an Abelian flavor symmetry. Such a model predicts CP -even and CP -odd Flavons that mediate FCNC at tree-level and thus can decay as $\phi \rightarrow tc$ ($\phi = H_F, A_F$), which is the focus of our work. We found the region of the parameter space consistent with both experimental and theoretical constraints. Then, we define a few benchmark points to evaluate the $\phi \rightarrow tc$ decays

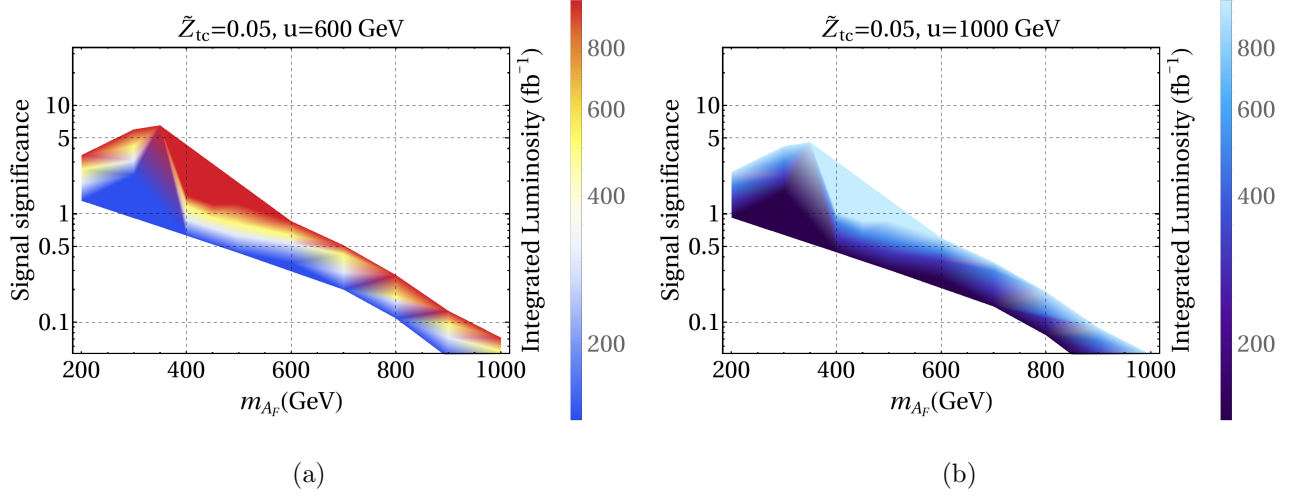


FIG. 12: Contour plots for the signal significance as a function of the integrated luminosity and the CP -odd flavon mass, m_{A_F} .

along with the flavon ϕ production cross-section at the LHC and its next stage, the HL-LHC. We present a Monte Carlo analysis of both the signal $gg \rightarrow \phi \rightarrow tc \rightarrow b\ell\nu_\ell c$ and the main standard model background, focusing on integrated luminosities in the range $140 - 1000 \text{ fb}^{-1}$, which allow us to assess the possibility that this channel could be detected at the LHC in the best scenario of the model parameters. However, with the advent of the HL-LHC operating to $\mathcal{L} \sim 1000 \text{ fb}^{-1}$, it could be possible to detect the decays $\phi \rightarrow tc$ for a reasonable scenario in the $200 < m_{A_F} < 700$ GeV interval and $200 < m_{H_F} < 380$ GeV. However, if one considers the expected integrated luminosity at the HL-LHC (3000 fb^{-1}), the mass interval of the Flavons could be increased. We make available, upon request, the necessary files to reproduce the Monte Carlo analysis.

ACKNOWLEDGEMENT

We acknowledge support from CONACYT (México). Partial support from VIEP-BUAP is also acknowledge. The work of M. A. Arroyo-Ureña was supported by Centro Interdisciplinario de Investigación y Enseñanza de la Ciencia (CIEC).

-
- [1] G. Aad *et al.* [ATLAS], Phys. Lett. B **716** (2012), 1-29 doi:10.1016/j.physletb.2012.08.020 [arXiv:1207.7214 [hep-ex]].
 - [2] S. Chatrchyan *et al.* [CMS], Phys. Lett. B **716** (2012), 30-61 doi:10.1016/j.physletb.2012.08.021 [arXiv:1207.7235 [hep-ex]].

- [3] J. G. Korner, A. Pilaftsis and K. Schilcher, Phys. Rev. D **47** (1993), 1080-1086 doi:10.1103/PhysRevD.47.1080 [arXiv:hep-ph/9301289 [hep-ph]].
- [4] J. L. Diaz-Cruz and J. J. Toscano, Phys. Rev. D **62** (2000), 116005 doi:10.1103/PhysRevD.62.116005 [arXiv:hep-ph/9910233 [hep-ph]].
- [5] T. Han and D. Marfatia, Phys. Rev. Lett. **86** (2001), 1442-1445 doi:10.1103/PhysRevLett.86.1442 [arXiv:hep-ph/0008141 [hep-ph]].
- [6] K. A. Assamagan, A. Deandrea and P. A. Delsart, Phys. Rev. D **67** (2003), 035001 doi:10.1103/PhysRevD.67.035001 [arXiv:hep-ph/0207302 [hep-ph]].
- [7] M. A. Arroyo-Ureña, J. L. Diaz-Cruz, E. Díaz and J. A. Orduz-Ducua, Chin. Phys. C **40** (2016) no.12, 123103 doi:10.1088/1674-1137/40/12/123103 [arXiv:1306.2343 [hep-ph]].
- [8] A. M. Sirunyan *et al.* [CMS], Phys. Rev. D **104** (2021) no.3, 032013 doi:10.1103/PhysRevD.104.032013 [arXiv:2105.03007 [hep-ex]].
- [9] K. Huitu, V. Keus, N. Koivunen and O. Lebedev, JHEP **05** (2016), 026 doi:10.1007/JHEP05(2016)026 [arXiv:1603.06614 [hep-ph]].
- [10] A. Lami and P. Roig, Phys. Rev. D **94** (2016) no.5, 056001 doi:10.1103/PhysRevD.94.056001 [arXiv:1603.09663 [hep-ph]].
- [11] E. Barradas-Guevara, J. L. Diaz-Cruz, O. Félix-Beltrán and U. J. Saldana-Salazar, [arXiv:1706.00054 [hep-ph]].
- [12] S. Chamorro-Solano, A. Moyotl and M. A. Pérez, J. Phys. G **45** (2018) no.7, 075003 doi:10.1088/1361-6471/aac458 [arXiv:1707.00100 [hep-ph]].
- [13] R. Primulando and P. Uttayarat, JHEP **05** (2017), 055 doi:10.1007/JHEP05(2017)055 [arXiv:1612.01644 [hep-ph]].
- [14] M. A. Arroyo-Ureña, J. L. Díaz-Cruz, G. Tavares-Velasco, A. Bolaños and G. Hernández-Tomé, Phys. Rev. D **98** (2018) no.1, 015008 doi:10.1103/PhysRevD.98.015008 [arXiv:1801.00839 [hep-ph]].
- [15] M. A. Arroyo-Ureña, T. A. Valencia-Pérez, R. Gaitán, J. H. Montes De Oca and A. Fernández-Téllez, JHEP **08** (2020), 170 doi:10.1007/JHEP08(2020)170 [arXiv:2002.04120 [hep-ph]].
- [16] G. Hernández-Tomé, J. I. Illana and M. Masip, Phys. Rev. D **102** (2020) no.11, 113006 doi:10.1103/PhysRevD.102.113006 [arXiv:2005.11234 [hep-ph]].
- [17] M. A. A. Ureña, R. Gaitan-Lozano, J. H. M. de Oca Yemha and R. S. Vélez, Rev. Mex. Fis. **67** (2021) no.4, 040801 doi:10.31349/RevMexFis.67.040801
- [18] J. L. Diaz-Cruz, M. A. Perez, G. Tavares-Velasco and J. J. Toscano, Phys. Rev. D **60** (1999), 115014 doi:10.1103/PhysRevD.60.115014 [arXiv:hep-ph/9903299 [hep-ph]].
- [19] A. Cordero-Cid, M. A. Perez, G. Tavares-Velasco and J. J. Toscano, Phys. Rev. D **70** (2004), 074003 doi:10.1103/PhysRevD.70.074003 [arXiv:hep-ph/0407127 [hep-ph]].
- [20] J. A. Aguilar-Saavedra, Acta Phys. Polon. B **35** (2004), 2695-2710 [arXiv:hep-ph/0409342 [hep-ph]].

- [21] A. Cordero-Cid, J. L. Garcia-Luna, F. Ramirez-Zavaleta, G. Tavares-Velasco and J. J. Toscano, J. Phys. G **32** (2006), 529-546 doi:10.1088/0954-3899/32/4/010 [arXiv:hep-ph/0501060 [hep-ph]].
- [22] C. Kao, H. Y. Cheng, W. S. Hou and J. Sayre, Phys. Lett. B **716** (2012), 225-230 doi:10.1016/j.physletb.2012.08.032 [arXiv:1112.1707 [hep-ph]].
- [23] A. Papaefstathiou and G. Tetlalmatzi-Xolocotzi, Eur. Phys. J. C **78** (2018) no.3, 214 doi:10.1140/epjc/s10052-018-5701-8 [arXiv:1712.06332 [hep-ph]].
- [24] M. Aaboud *et al.* [ATLAS], Phys. Rev. D **98** (2018) no.3, 032002 doi:10.1103/PhysRevD.98.032002 [arXiv:1805.03483 [hep-ex]].
- [25] M. A. Arroyo-Ureña, R. Gaitán, E. A. Herrera-Chacón, J. H. Montes de Oca Y. and T. A. Valencia-Pérez, JHEP **07** (2019), 041 doi:10.1007/JHEP07(2019)041 [arXiv:1903.02718 [hep-ph]].
- [26] P. Gutierrez, R. Jain and C. Kao, Phys. Rev. D **103** (2021) no.11, 115020 doi:10.1103/PhysRevD.103.115020 [arXiv:2012.09209 [hep-ph]].
- [27] B. Altunkaynak, W. S. Hou, C. Kao, M. Kohda and B. McCoy, Phys. Lett. B **751** (2015), 135-142 doi:10.1016/j.physletb.2015.10.024 [arXiv:1506.00651 [hep-ph]].
- [28] G. Apollinari, O. Brüning, T. Nakamoto and L. Rossi, CERN Yellow Rep. (2015) no.5, 1-19 doi:10.5170/CERN-2015-005.1 [arXiv:1705.08830 [physics.acc-ph]].
- [29] K. Tsumura and L. Velasco-Sevilla, Phys. Rev. D **81** (2010), 036012 doi:10.1103/PhysRevD.81.036012 [arXiv:0911.2149 [hep-ph]].
- [30] E. L. Berger, S. B. Giddings, H. Wang and H. Zhang, Phys. Rev. D **90** (2014) no.7, 076004 doi:10.1103/PhysRevD.90.076004 [arXiv:1406.6054 [hep-ph]].
- [31] J. L. Diaz-Cruz and U. J. Saldaña-Salazar, Nucl. Phys. B **913** (2016), 942-963 doi:10.1016/j.nuclphysb.2016.10.018 [arXiv:1405.0990 [hep-ph]].
- [32] M. Bauer, T. Schell and T. Plehn, Phys. Rev. D **94** (2016) no.5, 056003 doi:10.1103/PhysRevD.94.056003 [arXiv:1603.06950 [hep-ph]].
- [33] A. Bolaños, J. L. Diaz-Cruz, G. Hernández-Tomé and G. Tavares-Velasco, Phys. Lett. B **761** (2016), 310-317 doi:10.1016/j.physletb.2016.08.029 [arXiv:1604.04822 [hep-ph]].
- [34] A. M. Sirunyan *et al.* [CMS], Eur. Phys. J. C **79** (2019) no.5, 421 doi:10.1140/epjc/s10052-019-6909-y [arXiv:1809.10733 [hep-ex]].
- [35] R. L. Workman *et al.* [Particle Data Group], PTEP **2022** (2022), 083C01 doi:10.1093/ptep/ptac097
- [36] B. Abi *et al.* [Muon g-2], Phys. Rev. Lett. **126** (2021) no.14, 141801 doi:10.1103/PhysRevLett.126.141801 [arXiv:2104.03281 [hep-ex]].
- [37] C. Bonilla, D. Sokolowska, N. Darvishi, J. L. Diaz-Cruz and M. Krawczyk, J. Phys. G **43** (2016) no.6, 065001 doi:10.1088/0954-3899/43/6/065001 [arXiv:1412.8730 [hep-ph]].
- [38] C. D. Froggatt and H. B. Nielsen, Nucl. Phys. B **147** (1979), 277-298 doi:10.1016/0550-3213(79)90316-X

- [39] P. Mandrik [FCC study Group], J. Phys. Conf. Ser. **1390** (2019) no.1, 012044 doi:10.1088/1742-6596/1390/1/012044 [arXiv:1812.00902 [hep-ex]].
- [40] M. A. Arroyo-Ureña, R. Gaitán and T. A. Valencia-Pérez, Rev. Mex. Fis. E **19** (2022) no.2, 020206 doi:10.31349/RevMexFisE.19.020206 [arXiv:2008.00564 [hep-ph]].
- [41] A. Belyaev, N. D. Christensen and A. Pukhov, Comput. Phys. Commun. **184** (2013), 1729-1769 doi:10.1016/j.cpc.2013.01.014 [arXiv:1207.6082 [hep-ph]].
- [42] A. Semenov, Comput. Phys. Commun. **201** (2016), 167-170 doi:10.1016/j.cpc.2016.01.003 [arXiv:1412.5016 [physics.comp-ph]].
- [43] M. A. Arroyo-Ureña, A. Chakraborty, J. L. Díaz-Cruz, D. K. Ghosh, N. Khan and S. Moretti, [arXiv:2205.12641 [hep-ph]].
- [44] J. Gao, M. Guzzi, J. Huston, H. L. Lai, Z. Li, P. Nadolsky, J. Pumplin, D. Stump and C. P. Yuan, Phys. Rev. D **89** (2014) no.3, 033009 doi:10.1103/PhysRevD.89.033009 [arXiv:1302.6246 [hep-ph]].
- [45] J. Alwall, M. Herquet, F. Maltoni, O. Mattelaer and T. Stelzer, JHEP **06** (2011), 128 doi:10.1007/JHEP06(2011)128 [arXiv:1106.0522 [hep-ph]].
- [46] C. Degrande, C. Duhr, B. Fuks, D. Grellscheid, O. Mattelaer and T. Reiter, Comput. Phys. Commun. **183** (2012), 1201-1214 doi:10.1016/j.cpc.2012.01.022 [arXiv:1108.2040 [hep-ph]].
- [47] T. Sjöstrand, S. Ask, J. R. Christiansen, R. Corke, N. Desai, P. Ilten, S. Mrenna, S. Prestel, C. O. Rasmussen and P. Z. Skands, Comput. Phys. Commun. **191** (2015), 159-177 doi:10.1016/j.cpc.2015.01.024 [arXiv:1410.3012 [hep-ph]].
- [48] E. Conte, B. Fuks and G. Serret, Comput. Phys. Commun. **184** (2013), 222-256 doi:10.1016/j.cpc.2012.09.009 [arXiv:1206.1599 [hep-ph]].
- [49] J. de Favereau *et al.* [DELPHES 3], JHEP **02** (2014), 057 doi:10.1007/JHEP02(2014)057 [arXiv:1307.6346 [hep-ex]].
- [50] M. Cacciari, G. P. Salam and G. Soyez, Eur. Phys. J. C **72** (2012), 1896 doi:10.1140/epjc/s10052-012-1896-2 [arXiv:1111.6097 [hep-ph]].
- [51] M. Cacciari, G. P. Salam and G. Soyez, JHEP **04** (2008), 063 doi:10.1088/1126-6708/2008/04/063 [arXiv:0802.1189 [hep-ph]].